

**ABSTRACT**

Rare earth pyrochlores (A<sub>2</sub>B<sub>2</sub>O<sub>7</sub>) have shown improved performance over standard yttria stabilized zirconia (YSZ) with low thermal conductivity, better phase stability and improved resistance to infiltration of CMAS (calcium magnesium aluminosilicates). However, due to lower coefficient of thermal expansion (CTE) and lower fracture toughness has limited the use of pyrochlores. Drawbacks of single layer configuration can be overcome by multilayer configuration with conventional YSZ along with pyrochlore. Present study uses four configurations of TBC including single and multilayer produced with suspension plasma spraying. However, two samples with bi-layer configuration having porosity former with dense top coat were prepared. Denser top coat provides fracture toughness and intermediate with polymer porosity former reduces conductivity to restrict CMAS penetration. Microstructural evaluation was done using scanning electron microscope (SEM) before and after isothermal oxidation for 20 hrs. Columnar microstructure with vertical cracks was observed, these cracks and pores reduce due to narrowing after oxidation whereas denser layer shows non-columnar microstructure. Porosity was measured using water intrusion and image scanning method. Thermal conductivity was obtained from laser flash analyzer. By weight gain and SEM analysis samples with porosity former show low weight gain and high porosity and thermal conductivity was observed low. Erosion rate of denser top layer was found lower compared to other specimens. Bi-layer TBC with intermediate porous layer and dense top coat found better performing among other configurations of TBC.

**KEYWORDS:** Lanthanum zirconate, isothermal oxidation, porosity, thermal conductivity, suspension plasma spray.

**INTRODUCTION**

Increasing demand of higher efficiency of gas turbine and combustion temperature has encouraged use of high operating temperature materials to withstand these higher temperatures [1]. However, an increase in operating temperature has limited the life of these materials because of degradation. Thermal barrier coating is one of the means to provide thermal insulation and increase life of these materials [2-5]. Thermal barrier coating comprises of a substrate which is to be protected from high temperature exposure. Bond coat (BC) improves adhesion strength between ceramic top coat and metallic substrate and a ceramic top coat (TC) provides insulation from high temperature exposure [6].

Operating at high temperature poses several problems such as phase instability, sintering, bond coat oxidation forming thermally grown oxides (TGO). For its low intrinsic thermal conductivity with high fracture toughness 7–8 wt. % Y<sub>2</sub>O<sub>3</sub> stabilized ZrO<sub>2</sub> (YSZ) has emerged as the best choice for top coat. But at higher temperature (>1200°C) it undergoes significant sintering with CMAS infiltration, which results in high thermally grown oxides leading to early failure [8-9]. Drawbacks of YSZ have opened the search for new materials without compromising with desirable properties like phase stability, high fracture toughness and low thermal conductivity. Among the available pyrochlores lanthanum zirconate (LZ) La<sub>2</sub>Zr<sub>2</sub>O<sub>7</sub> is one of the best choices for its low bulk thermal conductivity and phase stability [10].

Atmospheric plasma spray (APS), Electron beam physical vapor deposit (EB-PVD) and High velocity oxy fuel (HVOF) are the promising coating methods in present days. Because of its low thermal fatigue life and non-

columnar microstructure made APS less advantageous than other methods [11]. Whereas, EB-PVD and HVOF produces columnar structure with better life time but the process is complicated and deposition rate is low. Literature has revealed that suspension plasma spray (SPS) is one of the attractive methods with high coating rate, high phase stability. SPS uses nano or submicrons sized powder suspended in a solvent which act as carrier. SPS produces a unique columnar microstructure with high porosity to resist oxygen penetration which considerably reduces formation of TGO[13].

The present work uses a multilayer TBC approach. Single layer TBC with top coat as YSZ coated with SPS and a single layer with top coat as LZ. Double layered TBC with YSZ on bond coat along with LZ on top of YSZ, another double layer TBC with LZ on bond coat over which YSZ. One more double layer configuration with YSZ mechanically mixed with polymer porosity formers coated on bond coat over which a thick dense layer of LZ was coated using SPS and LZ mixed with porosity formers coated on bond coat with dense YSZ coated on top of LZ [12].

Suspension plasma spray is the emerging coating process and has gained more impotence because of its unique columnar microstructure. It uses nano or submicron size powder which is mixed with a solvent generally ethanol or water which acts as carrier. A stream of carrier along with ceramic powder is made to enter into plasma flame. The flame along with ceramic powder is targeted to the substrate to deposit coating [13].

## EXPERIMENTAL METHODS

### Sample production

Present work uses nickel based Hastelloy superalloy as substrate material. Specimens were plates of 25mm×25mm×1.54mm for microstructural analysis and 50mm×40mm×6mm for isothermal oxidation. Thickness of specimens for microstructure study was kept thin (1.54mm) to facilitate the ease of preparation and projection under Scanning electron microscope (SEM). Specimens were grit blasted with alumina particles of abrasive size of 220 to produce rough surface on substrate. The roughness produced by grit blasting was 5µm on Ra scale, roughness produced enhances adhesion between substrate and bond coat. The bond coat selected was NiCoCrAlY composition deposited using high velocity air fuel (HVOF) and a thickness of 200±30µm was kept same for all specimens. Six types of coatings were produced with two specimens for every coating type. Single layer and Bi-layer coating samples S1 and S2, were prepared by standard suspension coating method explained in this paper. Specimen S3 and S4 were produced with intermediate layer LZ/YSZ mixed with polymer porosity formers (At metalizing equipment, Bangalore). Samples prepared for the present study are shown in figure 1

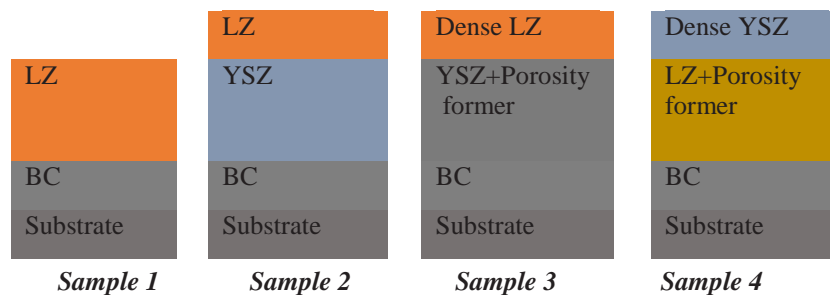


Figure 1: Multilayer TBC configuration

### Suspension plasma spray

Suspensions plasma spray uses solvent which act as carrier and ceramic powder (Nano or micron ceramic powder) as solute[14]. In present work ethanol is used as solvent with solute being 7% YSZ having a median particle size of 500nm, another suspension prepared with ethanol and LZ at AUM technologies (Bangalore, India). Due to the complexity of process, a number of parameters of SPS kept constant in present study. Suspensions are fed in to plasma flame with help of atomizer to form small droplets which are accelerated towards substrate to form coating and solvent gets evaporated. Process parameters used in present study are listed in table.1 [15]

<i>Parameters</i>	<i>Sample 1</i>	<i>Sample 2</i>	<i>Sample 3</i>	<i>Sample 4</i>
Power	220A	220A	220A	220A
Spraying distance	100mm	90mm	90mm	90mm
Suspension density?(g/cc)	1.18	1.3	2.15	2.1
Feed rate ml/min	45ml/min	50ml/min	50ml/min	50ml/min
Deposition rate( $\mu\text{m/pass}$ )	3	3.5	5.8	5.8

*Table 1: Process parameters of suspension plasma spray*

### **Isothermal oxidation test**

Isothermal oxidation is a lifetime testing technique that primarily assesses oxidation driven failure in a TBC system. The TBC specimens with single layered and bi-layered were placed in electric furnace for various length of time in air environment at 1200°C. Isothermal oxidation test conditions in this study are chosen to simulate the actual working condition where oxidation is aggressive in nature with temperature (1200°C). Specimens were heated at 100°C/hour and left in furnace at cooling rate of 100°C/hour. The possible reasons for cooling specimens in furnace after oxidation could be to avoid thermal residual stresses [16-17].

### **Microstructure**

Microstructure of specimens is analyzed after the 20hours of isothermal oxidation. Specimens prepared according standard procedure of preparation. Specimens were cut using slow speed diamond cutting blade and cold mounted by a 5:1 combination of epoxy resin & hardener. Polishing was carried out on revolving discs of 220grit, 120grit successively [19]. Further sectioned and polished specimens were polished with diamond paste and with help of 0.05 micronsilica paste a scratch free mirror finished was obtained. Thickness of single layered and bi-layered coating and thermally grown oxides (TGO) were measured by locating 15 points on cross section and using optical microscope. Scanning electron microscope (Hitachi, TM3000 model) was used to analyze the microstructure of multilayered TBC [20].

### **Porosity Measurement**

Porosity plays an important role in thermal property and life time of TBCs, as pores media retards the oxygen penetration causing low oxidation leading to improved life time. Present study carried out water intrusion method and image analysis to compare and estimate the porosity of samples before oxidation and after oxidation.

**Water intrusion:** It is one of simplest method to determine the porosity which estimates open pores as water cannot infiltrate closed and isolated pores. Free standing TBCs are dissolved in HNO<sub>3</sub> solution and dried in oven at 150°C for 30min to remove liquid from pores. Samples were vacuumed several times to remove air and immersed in water and allow water to infiltrate the pores of coating. After removing from water final weight of samples was recorded and compared with initial weight to estimate the percent of porosity.

**Image analysis to estimate porosity:** Porosity of TBCs estimated by SEM image analysis at 800X (using SEM) is compared with the porosity obtained from water intrusion. In this procedure images were taken along the cross section of coating and then processed with image analysis software. Image analysis can estimate the closed and isolated pores, higher image resolution facilitate to identify smallest size pores. Individual layer porosity can be estimated with the help of software. However, the software does not account the columnar gaps and cracks at higher magnification which leads estimate less porosity as compared to water intrusion method shown in fig.

**Weight gain or loss analysis:** Weight loss or gain method determines the amount of oxidation occurred during high temperature exposure. The procedure include weighing of samples before oxidation with sensitive weighing apparatus (K Roy DJ602) after the different exposure time the final weight of all samples was measured. The difference in initial and final weight gives the approximate oxidation of samples.

**Thermal properties:** Thermal conductivity and thermal diffusivity of all samples were tested after isothermal oxidation for 20hr using Laser Flash Analyzer (LFZ) NETZSCH 467. The results are plotted for all samples to compare the changes due to position of different layers. The procedure includes cutting of oxidized samples using water jet and coated with graphite to improve laser light absorption ability. Rare end of sample exposed to laser of known impulse and record the rise in temperature. Response of the sample for temperature rise was normalized and thermal diffusivity was calculated using equation 1.

$$\alpha = (0.1388 * d^2) / t_{0.5} \quad (1)$$

Thermal conductivity was estimated using equation 2. Specific heat was calculated using scanning calorimeter 404C which uses Sapphire as reference.

$$k = \alpha(T) * c_p(T) * \rho(T) \quad (2)$$

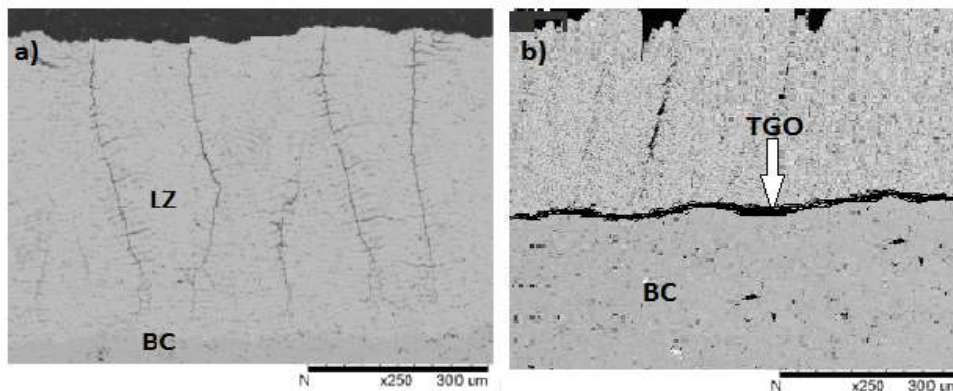
### Erosion Test

Erosion testing was performed according to standard erosion testing method at metalizing equipment center. The uses a standard polycarbonate piece as reference. The abrasive of alumina of 50 $\mu$ m was used which was blast feeded through the nozzle at very high velocity. The blast nozzle was set at 60 degrees to the specimen surface at a distance 5cm. Testing was carried out for 50seconds until the grit blast removes the material. After the erosion test the depth of pit formed by erosion was calibrated using micrometer gauge. Erosion test was carried out for minimum of samples to evaluate accurate erosion rate.

## RESULTS AND DISCUSSIONS

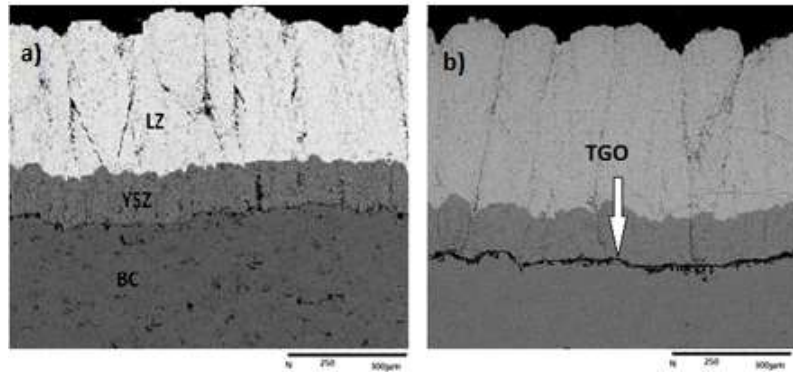
### Microstructure Evaluation

Micrographs of all coatings produced are displayed by performing previously mentioned method; microstructure analysis was done on polished cross-sections using the SEM as shown in Figure 2. Previous researchers have revealed with decrease in the particles size of ceramic powder, a regular and periodic columnar structure can be generated which justifies the micrographs presented in this work. The average thickness of bond coat was 200 $\mu$ m  $\pm$  20 $\mu$ m deposited using HVOF. The top YSZ and LZ layer were 300 $\mu$ m to 350 $\mu$ m. Figure 2(a&b) represents the Single layer LZ coated on bond coat. Micrograph shows regular columnar structure which was produced by keeping solid feed rate of 25%. Figure 3(a&b) shows the top layer with LZ coated on YSZ which is coated on bond coat having same thickness as of LZ coating deposited by keeping same feed rate. Average column width in both YSZ and LZ shows the same of 60 $\pm$ 6 $\mu$ m. Density of columns in YSZ coating is 10 $\pm$ 3 columns/mm. LZ coating has high density of 15 $\pm$ 2 columns/mm the possible reason can be due the low friction in particles of LZ. Figure 2(a) and (b) represents micrographs of Single layer TBC sintered for 20hours isothermally. The samples showed ceramic topcoat microstructures with initiation of vertical crack opening which is caused by the stresses developed by the growth of TGO. Horizontal cracks along the TGO were seen in both Single and bi-layer coated samples. Average TGO thickness in LZ ceramic was 9.23 $\mu$ m and in Bi-layer sample showed reduced TGO with 4.1 $\mu$ m. the possible reason for the reduced TGO in LZ can be for high fracture toughness of LZ 175GPa.



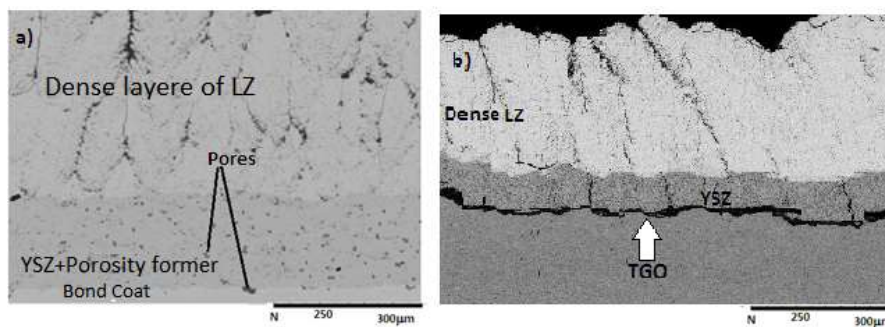
**Figure 2: Single layer with TC as LZ a) Before oxidation b) After oxidation for 20hr**

Figure 3: shows the bi-layer TBC system having top coat as LZ deposited on YSZ deposited using SPS method. Micrographs of both bi-layer system were displayed using SEM. Thickness of both intermediate layers were kept same of 200 $\mu$ m. Bi-layer TBC's LZ on YSZ shown high columnar gaps and porosity before heat treatment which reduces after isothermal oxidation for 20hrs. TGO growth of 5.6 $\pm$ 1 $\mu$ m was observed in TBC with LZ as top coat. The possible reasons for that can be higher penetration of oxygen and high conduction of heat through the YSZ.



**Figure 3: Bi-Layer with TC as LZ/YSZ a) Before oxidation b) After oxidation for 20hr**

Cross-sectional micrographs of samples with bi-layer configuration having dense top layer with intermediate layer with porosity former are shown in figure 4 and 5. Dense layered top coat restricts the penetration of CMAS and forms a protective layer to avoid oxidation which results in low formation of TGO layer. Porosity before sintering was observed to have 21 to 29% which further reduced after heat treatment to about 19-24%. TBC with top layer as dense LZ show low TGO due formation  $Al_2O_3$  and  $Cr_2O_3$  protective oxide layer to restrict penetration of oxygen in to metallic bond coat. Sudden drop in porosity after sintering was observed for specimens S5 and S6 due burn off of polymer porosity former. Thick top layer acts as erosion resisting layer and intermediate porous layer reduces growth of TGO.



**Figure 4: Bi-Layer having intermediate layer with porosity former along with top LZ/YSZ a) Before oxidation b) After oxidation for 20hr**

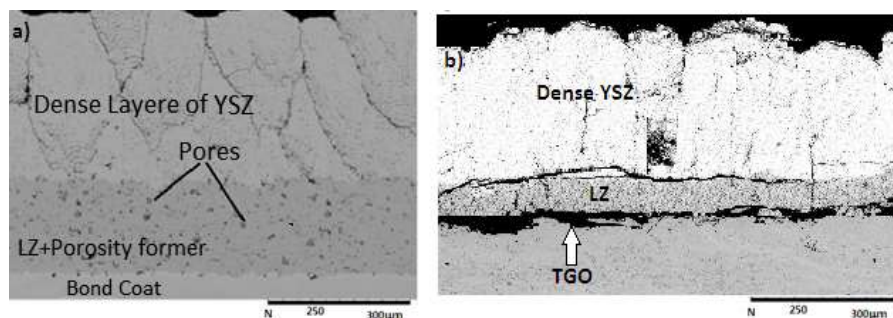


**Figure 5: Bi-Layer having intermediate layer with porosity former along with YSZ/LZ a) Before oxidation b) After oxidation for 20hr**

### Porosity

The procedure followed for quantitative assessment of porosity in the bond coat and in the ceramic layer followed as explained in earlier chapter. The study uses water intrusion method and image analysis to estimate the porosity.

### Water Intrusion Method

This method uses free standing coatings to measure only the open pores and cracks as water cannot infiltrate pores which are hidden and isolated. Results of porosity by water intrusion method are plotted along with the image

analysis before isothermal oxidation and after isothermal oxidation for 20hours. The results showed high porosity before oxidation for all samples and reduces after oxidation, possible reason for that can be closure of pores causing reduction porosity. Porosity of single layer TBC with LZ/YSZ as top coat estimated to 16 to 20%. Bi-layer TBC with dense LZ on top followed by YSZ coated with porosity formers show high porosity of 29% which after sintering reduces to 24%. Porosity formers burn off to create high porosity during high temperature exposure.

**Image Analysis**

Porosity values and ranking of all samples obtained from image analysis at 1000X are different from values and ranking from water intrusion method as shown in Figure. 6. Image analysis can estimate porosity total porosity including column gaps and pores provided the resolution should be high enough to identify the smallest pore. Present study uses software which does not considers vertical crack and column gaps in account as it requires high magnification. These column gaps and vertical cracks contribute lot to total porosity, which is why porosity low by image analysis as compared to water intrusion method.

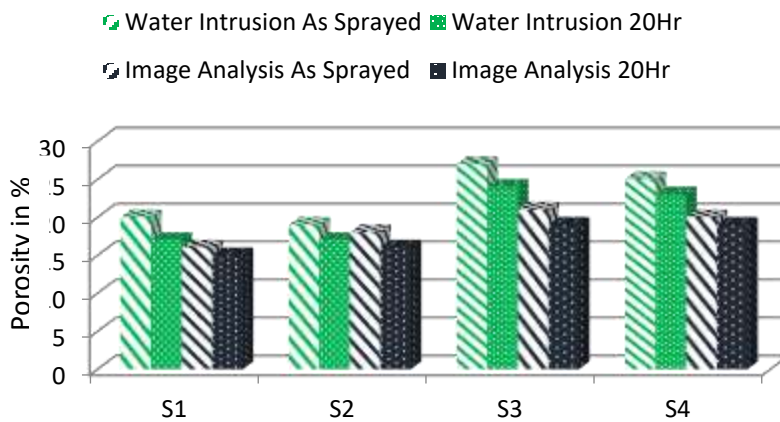


Figure 6: Porosity estimated using Water intrusion and image analysis

**Weight gain/loss analysis.**

Weight gain/loss analysis was performed to understand the oxidation rate of individual specimens as explained earlier [17]. Weight gain results of six different TBC systems (Single, Bi layer and Bi-layer with porosity formers) exposed to 1200°C for 20hours of oxidation are plotted in Figure 7. A common trend of gain in weight of all samples was observed. Weight gain by single layer TBC with both top coat as YSZ and LZ showed higher weight gain compared to other Bi-layer systems. However, in case of both Bi-layer configurations specimen S3 and S4 showed less weight gain due to the readily available protective oxide layer formed by elements (Al and Cr). These passive protective oxide layers (Al<sub>2</sub>O<sub>3</sub> and Cr<sub>2</sub>O<sub>3</sub>) help in resisting further oxidation of the underlying metal.

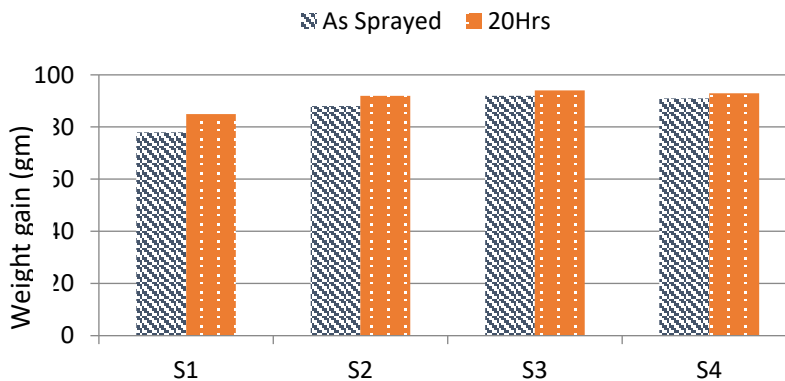


Figure 7: Weight gain plot of all investigated samples after isothermal oxidation test at 1200°C for 0 h and 20 h.

Weight gain analysis concluded that specimens with single layer show high oxidation rate as compared to double layered configuration. Bi-layer with intermediate layer with porosity formers gained less amount of weight due to burn out of polymer porosity formers and forming passive protective layer for oxygen penetration.

**Thermal conductivity**

Thermal conductivity of all specimens before and after 20hours of oxidation is plotted in figure 8. A trend of increase in thermal conductivity of all specimens after 20hours isothermal oxidation was observed as shown in figure 10. The possible reason for increase in thermal conductivity after oxidation can be attributed towards the narrowing of pores and cracks due effect of sintering. Specimen S3 and S4 records least thermal conductivity of 0.7 and 0.9 before heat treatment due to use of polymer porosity former. However, due to heat treatment the porosity former burn off and thermal conductivity as increased slightly more than other specimens.

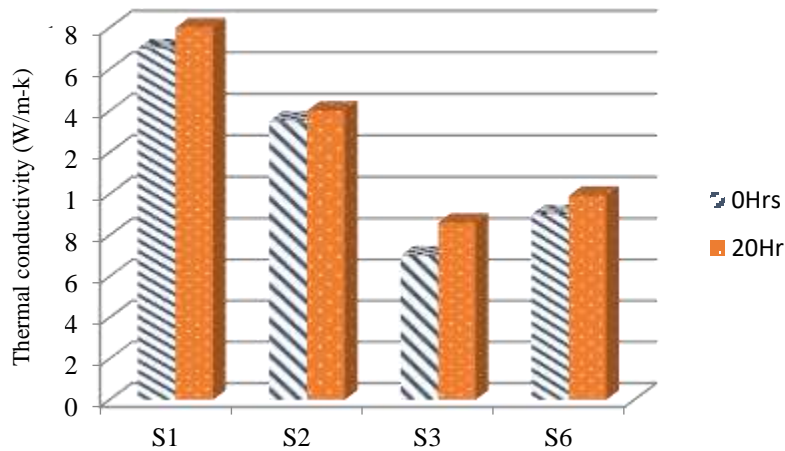


Figure 8: Thermal conductivity before and after 20hr of oxidation

**Erosion Rate**

Erosion rate data is shown in figure 9. Micrometer was used to calibrate pit generate due to erosion and same steps were followed as used to measure surface roughness. To evaluate accurate erosion rate test was carried out on all 4 specimens at three spots before oxidation. Single layer specimens show high erosion as compared to all other specimens. S3 and S4 show less erosion rate due dense layer present at the top. Samples prepared with less suspension density forms less dense top coat. Whereas, the specimens coated with high suspension density show dense layer and leads to low erosion rate.

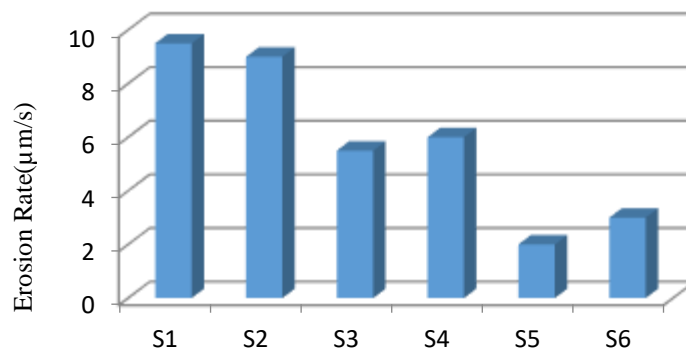


Figure 9: Erosion rate in µm/s

**CONCLUSION**

Different configuration of multilayered thermal barrier coating with lanthanum zirconate(LZ)/YSZ were prepared using suspension plasma spraying. Effect of isothermal oxidation at 1200°C for 20hours on performance was analyzed and following conclusion were drawn

- Lanthanum Zirconate forms a low conductive TBC and has emerged as alternate for conventional YSZ. Use of porosity former has increased porosity with reduction in thermal conductivity as well as growth of TGO.
- Denser top can be achieved by increasing the suspension density, and denser layer acts as protective layer to prevent coating from erosion.
- Bi-layer configuration with porosity former and denser top layer with LZ and YSZ that is specimen S6 has emerged as better TBC with optimal operating performance

**Authors declare there are no conflicts of interest**

## REFERENCE

- [1] G. Mauer, M. O. Jarligo, D. E. Mack, and R. Vaßen, “Plasma-Sprayed Thermal Barrier Coatings: New Materials, Processing Issues, and Solutions,” *J. Therm. Spray Technol.*, vol. 22, pp. 646–658, Jun. 2013.
- [2] Pirzada, R. W. Grimes, and J. F. Maguire, “Incorporation of divalent ions in  $A_2B_2O_7$  pyrochlores,” *Solid State Ion.*, vol. 161, no. 1–2, pp. 81–91, Jul. 2003
- [3] P. Poza, J. Gomez-Garcia, and C. J. Munez, *Acta Mater.*, 60 [20] 7197–7206 (2012)
- [4] C. Mercer, S. Faulhaber, A. G. Evans, and R. Darolia, “A delamination mechanism for thermal barrier coatings subject to calcium–magnesium–alumino-silicate (CMAS) infiltration,” *Acta Mater.*, vol. 53, no. 4, pp. 1029–1039, Feb. 2005.
- [5] Satyapal Mahade, Nicholas Curry, Stefan Bjorklund, Nicolaie Markocsan, Per Nylén, “Thermal conductivity and thermal cyclic fatigue of multilayered  $Gd_2Zr_2O_7/YSZ$  thermal barrier coatings processed by suspension plasma spray,” 0.1016/j.surfcoat.2015.11.009
- [6] M. P. Schmitt, A. K. Rai, R. Bhattacharya, D. Zhu, and D. E. Wolfe, “Multilayer thermal barrier coating (TBC) architectures utilizing rare earth doped YSZ and rare earth pyrochlores,” *Surf.Coat. Technol.*, vol. 251, pp. 56–63, Jul. 2014
- [7] C. Wang, Y. Wang, L. Wang, G. Hao, X. Sun, F. Shan, and Z. Zou, “Nanocomposite Lanthanum Zirconate Thermal Barrier Coating Deposited by Suspension Plasma Spray Process,” *J. Therm. Spray Technol.*, vol. 23, no. 7, pp. 1030–1036, Feb. 2014
- [8] E. Bakan, D. E. Mack, G. Mauer, and R. Vaßen, “Gadolinium Zirconate/YSZ Thermal Barrier Coatings: Plasma Spraying, Microstructure, and Thermal Cycling Behavior,” *J. Am. Ceram. Soc.*, vol. 97, no. 12, pp. 4045–4051, Dec. 2014
- [9] Z. Xu, L. He, R. Mu, S. He, and X. Cao, “Preparation and characterization of  $La_2Zr_2O_7$  coating with the addition of  $Y_2O_3$  by EB-PVD,” *J. Alloys Compd.*, vol. 492, no. 1–2, pp. 701–705, Mar. 2010.
- [10] Z. Xu, L. He, R. Mu, S. He, and X. Cao, “Preparation and characterization of  $La_2Zr_2O_7$  coating with the addition of  $Y_2O_3$  by EB-PVD,” *J. Alloys Compd.*, vol. 492, no. 1–2, pp. 701–705, Mar. 2010.
- [11] R. Vassen, X. Cao, F. Tietz, D. Basu, and D. Stöver, “Zirconates as New Materials for Thermal Barrier Coatings,” *J. Am. Ceram. Soc.*, vol. 83, no. 8, pp. 2023–2028, Aug. 2000.
- [12] L. Wang, Y. Wang, X. G. Sun, J. Q. He, Z. Y. Pan, and C. H. Wang, “Thermal shock behavior of 8YSZ and double-ceramic-layer  $La_2Zr_2O_7/8YSZ$  thermal barrier coatings fabricated by atmospheric plasma spraying,” *Ceram. Int.*, vol. 38, no. 5, pp. 3595–3606, Jul. 2012
- [13] N. Curry, K. VanEvery, T. Snyder, J. Susnjär, and S. Bjorklund, “Performance Testing of Suspension Plasma Sprayed Thermal Barrier Coatings Produced with Varied Suspension Parameters,” *Coatings*, vol. 5, no. 3, pp. 338–356, Jul. 2015
- [14] P. Sokołowski, S. Kozerski, L. Pawłowski, and A. Ambroziak, “The key process parameters influencing formation of columnar microstructure in suspension plasma sprayed zirconia coatings,” *Surf. Coat. Technol.*, vol. 260, pp. 97–106, Dec. 2014
- [15] Z. Lu, S.-W. Myoung, Y.-G. Jung, G. Balakrishnan, J. Lee, and U. Paik, “Thermal Fatigue Behavior of Air-Plasma Sprayed Thermal Barrier Coating with Bond Coat Species in Cyclic Thermal Exposure,” *Materials*, vol. 6, no. 8, pp. 3387–3403, Aug. 2013.
- [16] A. Ganvir, N. Curry, S. Björklund, N. Markocsan, and P. Nylén, “Characterization of Microstructure and Thermal Properties of YSZ Coatings Obtained by Axial Suspension Plasma Spraying (ASPS),” *J. Therm. Spray Technol.*, pp. 1–10, Jun. 2015
- [17] Satyapal Mahade, Ran Li, Stefan Bjorklund, Nicolaie Markocsan, and Per Nylén “Isothermal Oxidation Behavior of  $Gd_2Zr_2O_7/YSZ$  Multilayered Thermal Barrier Coatings,” DOI:10.1111/ijac.12527



- [18] J. M. Drexler, A. L. Ortiz, and N. P. Padture, "Composition effects of thermal barrier coating ceramics on their interaction with molten Ca–Mg–Al–silicate (CMAS) glass," *Acta Mater.*, vol. 60, no. 15, pp. 5437–5447, Sep. 2012
- [19] S. V. U. A. V. Radha, "Thermochemistry of lanthanum zirconate pyrochlore," *J. Mater. Res.*, vol. 24, no. 11, pp. 3350 – 3357, 2009
- [20] K. S. Lee, D. H. Lee, and T. W. Kim, "Microstructure controls in Gadolinium Zirconate/YSZ double layers and their properties," *J. Ceram. Soc. Jpn.*, vol. 122, no. 1428, pp. 668–673, 2014
- [21] N. Curry, Z. Tang, N. Markocsan, and P. Nylen, "Influence of bond coat surface roughness on the structure of axial suspension plasma spray thermal barrier coatings — Thermal and lifetime performance," *Surf. Coat. Technol.*, vol. 268, pp. 15–23, Apr. 2015

### HIGHLIGHT

Article is successive part of previously published paper on multilayer Thermal barrier coating.

1 6 different configuration of multilayer TBC were prepared and checked for their isothermal behavior at 1200 C  
3 Porosity, thermal conductivity, weight gain and erosion test were carried out.

2. Configuration with pyrochlore La<sub>2</sub>Zr<sub>2</sub>O<sub>7</sub> along with polymer porosity former having dense top layer has shown better results with high porosity with less erosion